SUPPLEMENTARY FIGURES LEGENDS

Figure S1. Effect of ssDNA oligonucleotides on NHEJ activity in cell extracts.
A/ End-joining assay under standard reaction conditions with HeLa cell extracts, in the presence or not of DNA-PK specific inhibitor NU7441 (DNA-PKi) and ssO at the indicated concentration. DNA ligation products were separated by agarose gel electrophoresis followed by SYBR-Green staining. **B/** End-joining assay with extracts from HCT116 Lig4$^{-/-}$ cells, in the presence or not of DNA-PK specific inhibitor NU7441 (DNA-PKi) and ssO at the indicated concentration. **C/** End-joining assay with extracts from HCT116 Lig4$^{-/-}$ cells, in the presence or not of DNA-PK specific inhibitor NU7441 (DNA-PKi) and 4 µM of ssO or dsO, as indicated. **D/** End-joining assay with extracts from HeLa or HCT116 cells and linearized pDVG plasmid, in the presence or not of DNA-PK specific inhibitor NU7441 (DNA-PKi) and ssO, as indicated. **E/** Junction characterization after end-joining of linearized pDVG94 plasmid with extracts wild-type or Lig4$^{-/-}$ HCT116 cells. After ligation, plasmids were purified, the junction was PCR-amplified and digested by BstXI. Digestion products were separated by acrylamide gel electrophoresis followed by SYBR-Green staining. **F/** End-joining assay with extracts from HCT116 Lig4$^{-/-}$ cells, in the presence or not of ssO of various lengths, as indicated.

Figure S2. Length-dependent competition by ssO on Ku-binding to ds DNA ends in vitro. Electrophoretic mobility shift assay of ds biotinylated DNA probe incubated with purified human recombinant Ku protein, in the presence of competitor ssO of various lengths, as indicated.

Figure S3. Involvement of Lig3 in ssO-promoted end-joining *in vitro*. A/ western blot analysis of extracts from HeLa and HeLa shLig3 derivative cells (gift from D. Biard, CEA, France (1)). **B/** End-joining assay with extracts from HeLa and HeLa shLig3 derivative cells, in the presence or not of DNA-PK specific inhibitor NU7441 (DNA-PKi) and 4 µM of ssO, as indicated. **C/** End-joining assay with extracts from HeLa or HCT116 cells, in the presence or not of 4 µM of ssO, as indicated. The ssO-mediated end-joining stimulation was calculated as the ratio between the end-joining efficiency with and without ssO (NA, not applicable because for HCT116 DNA-PKcs$^{-/-}$ extracts, initial end-joining was null).

Figure S4. Effect of ssO on cell cycle. Cell cycle profiles of mock (control) or LNA ssO transfected HCT116 (left) and RPE-1 XRCC6+/- (right) cells. Flow cytometry was used to analyze the cell cycle distribution of cells transfected for 2 h and post-incubated 1 h in complete medium.

Figure S5. Relative kinetics of Ku recruitment at laser sites in control and ssO-treated cells. Data presented in Fig.4B were reanalyzed by setting at 100% the increase in Ku fluorescence intensity at laser site measured at the latest time point for each cell monitored.

1. Biard, D.S. (2007) Untangling the relationships between DNA repair pathways by silencing more than 20 DNA repair genes in human stable clones. *Nucleic Acids Res*, **35**, 3535-3550.

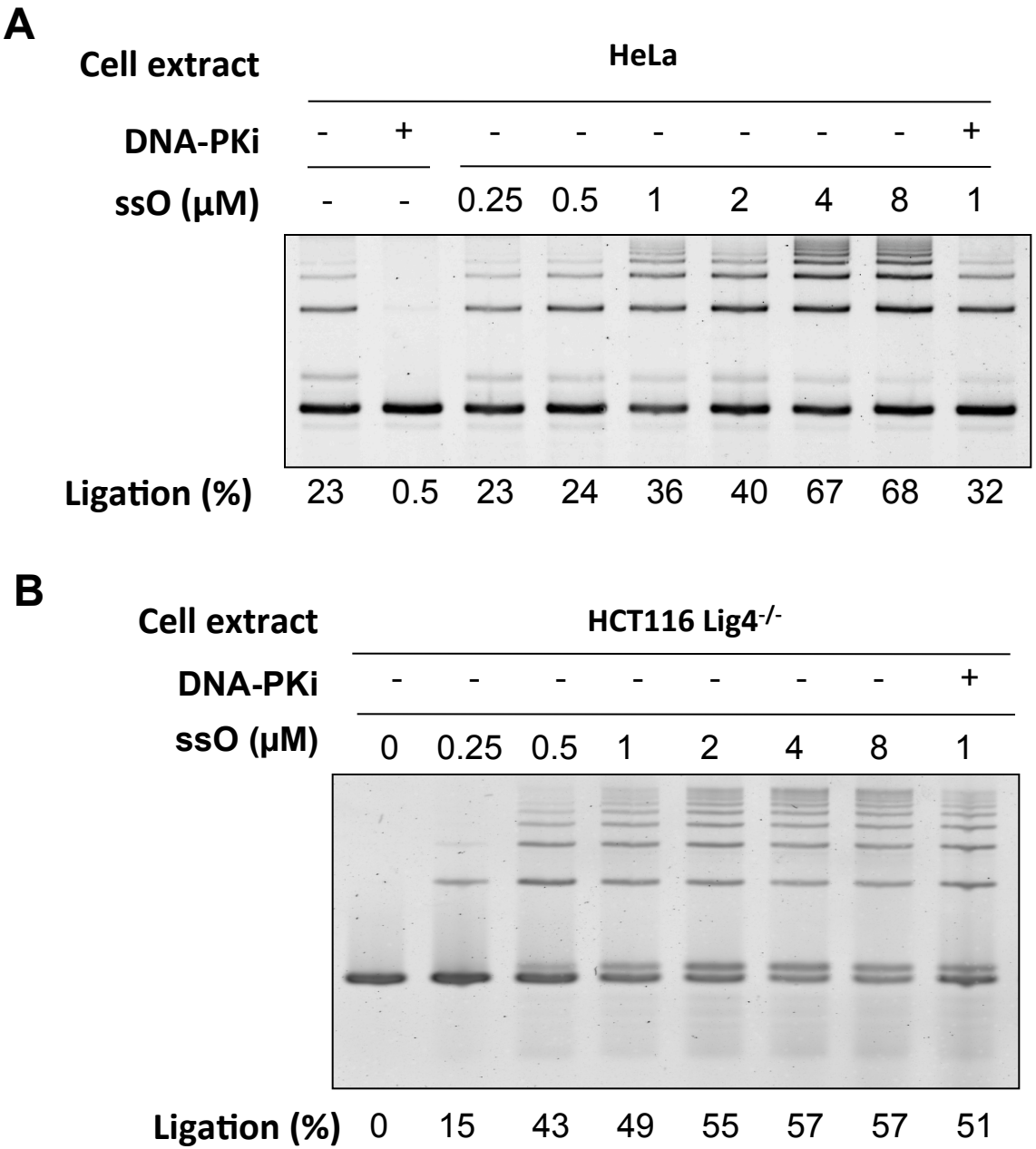

Sup Figure S1

C

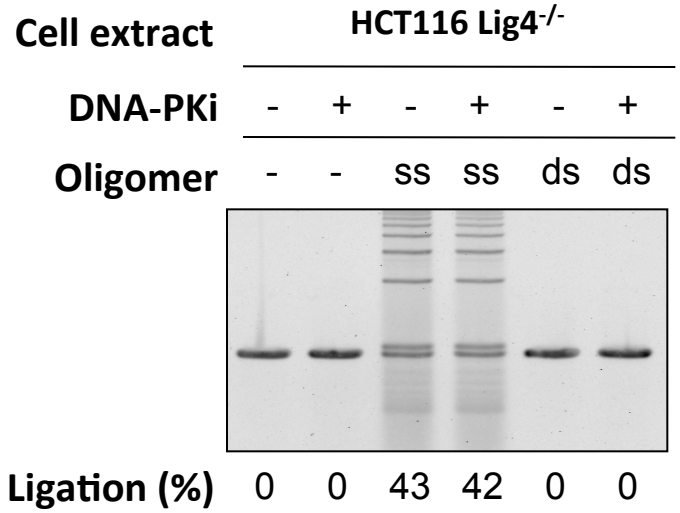

D

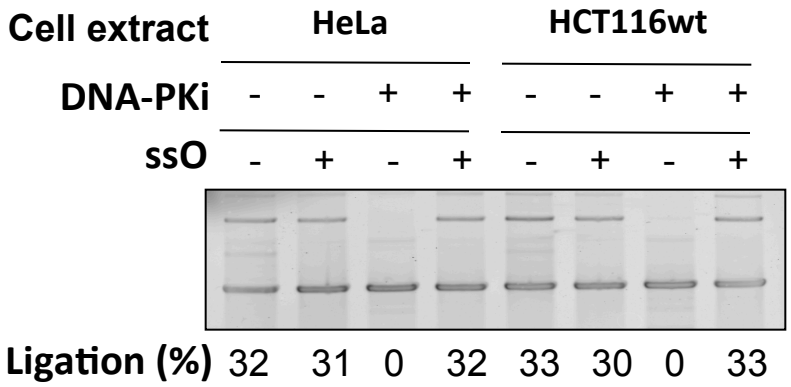

Sup Figure S1

E

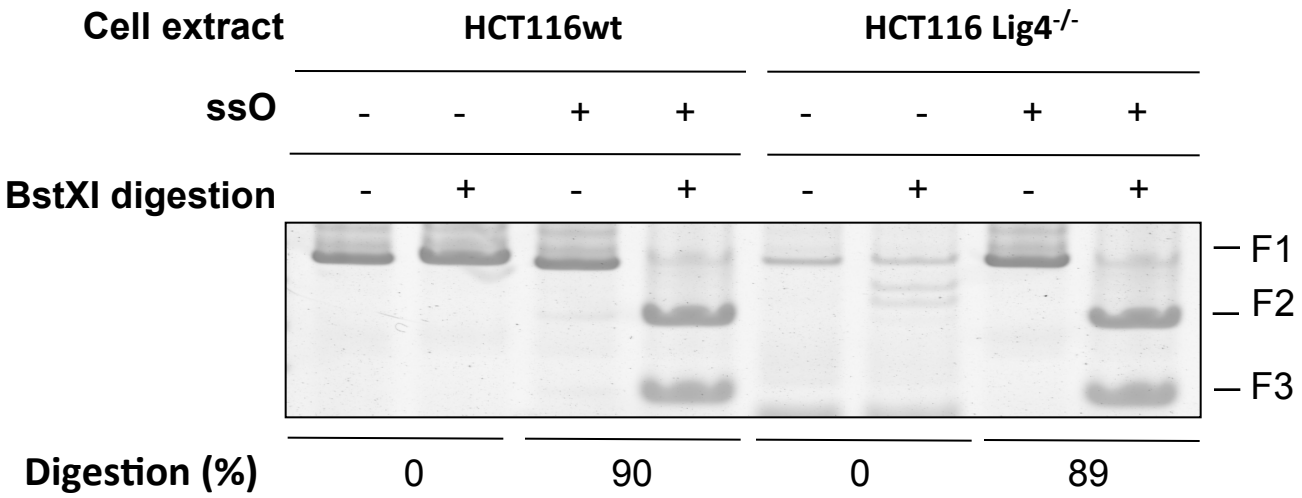

F

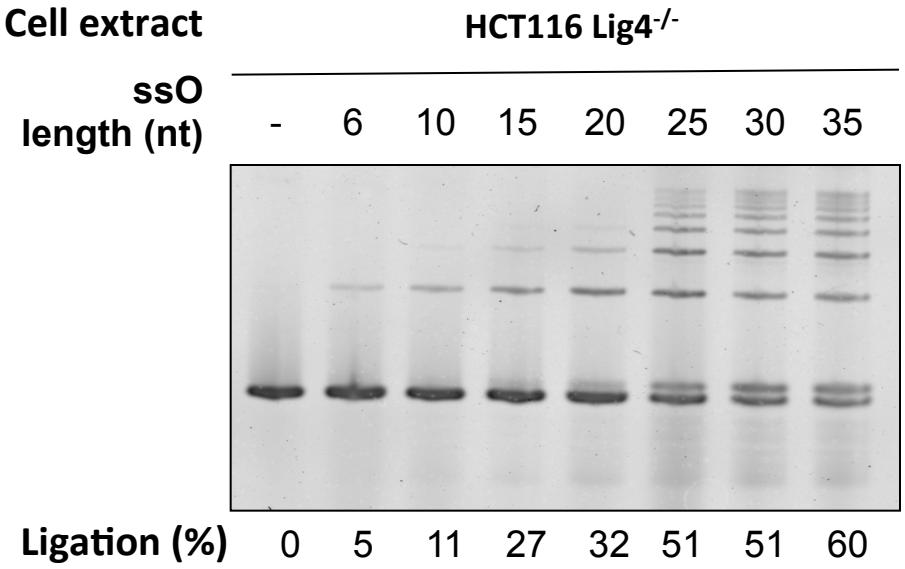

Sup Figure S1

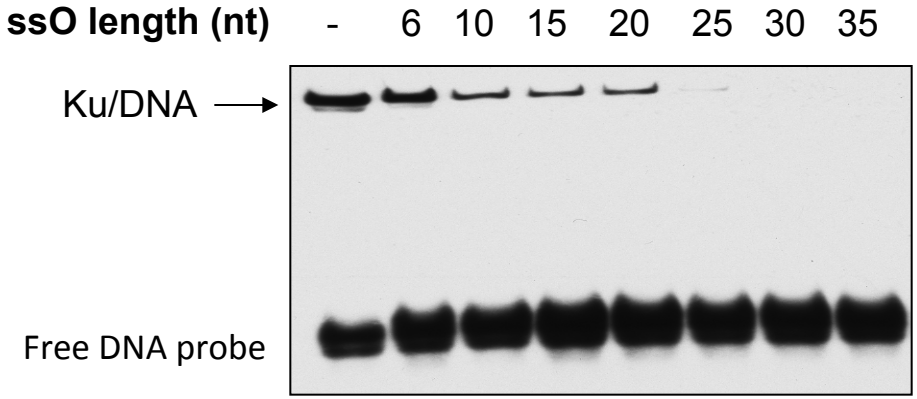

Sup Figure S2

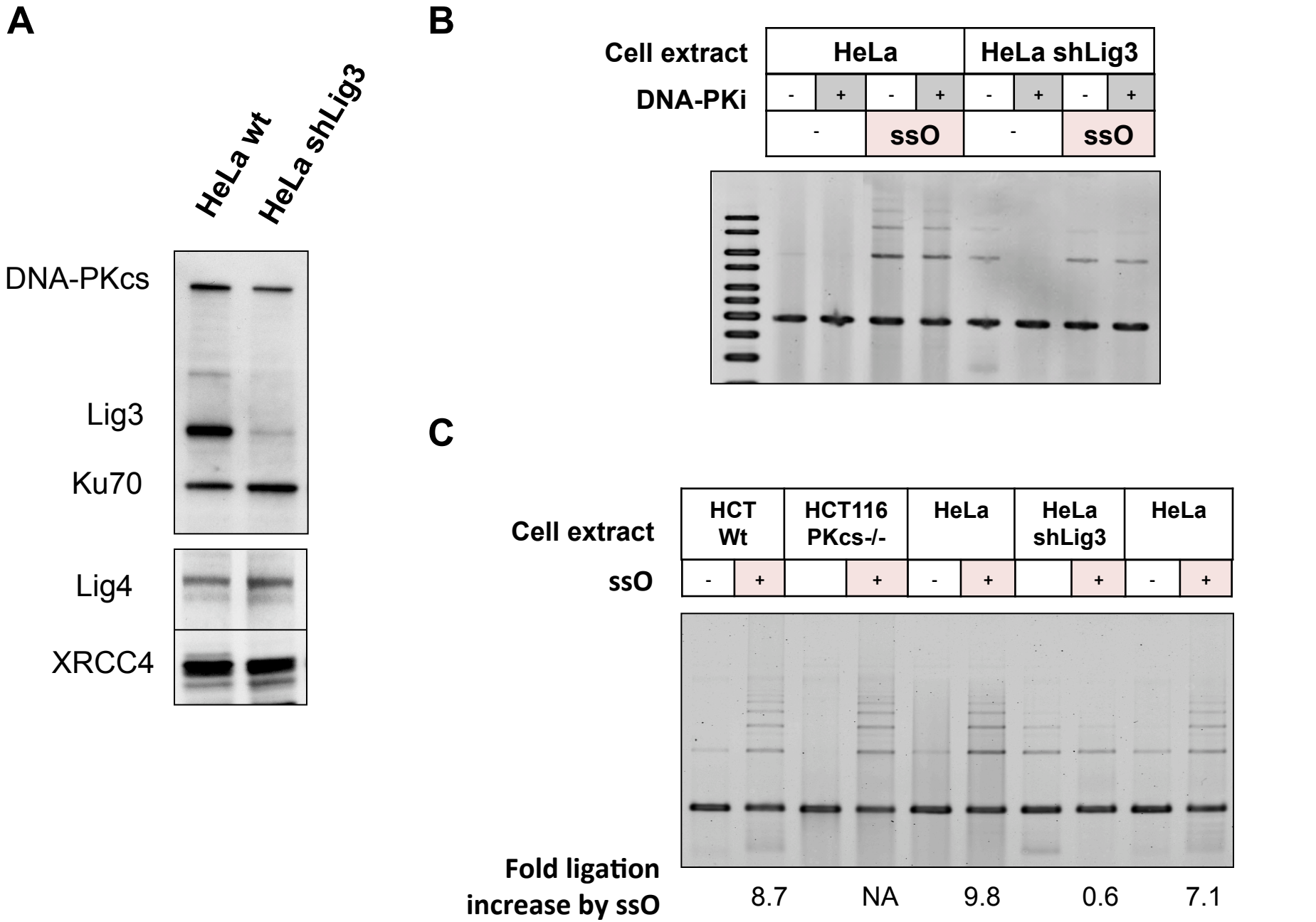

Sup Figure S3

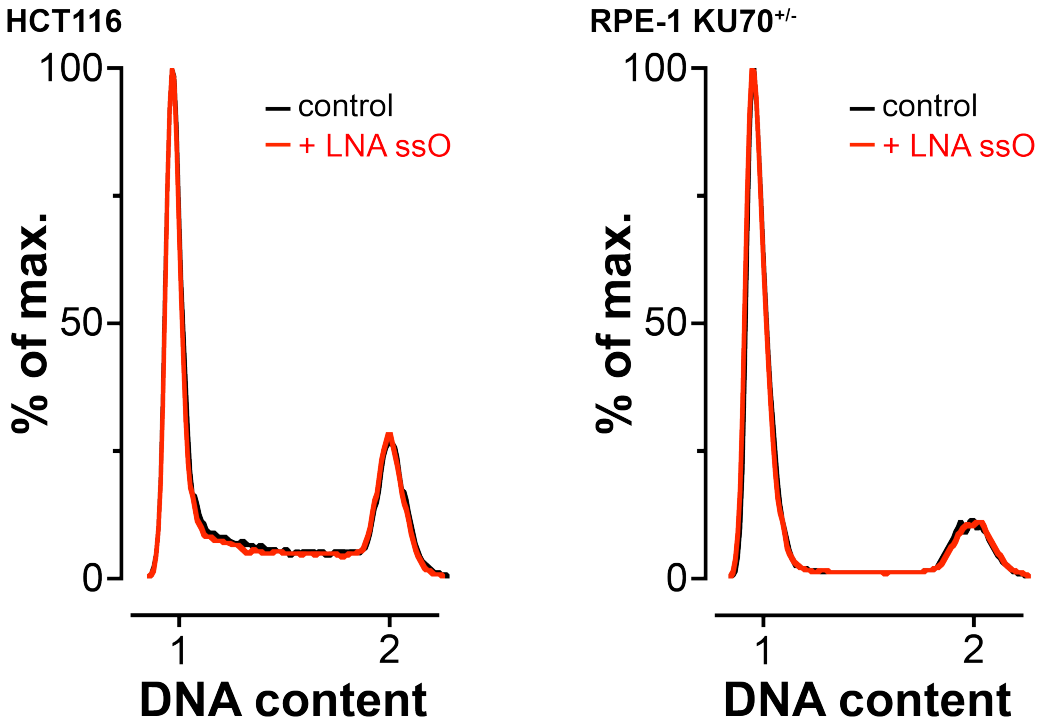

Sup Figure S4

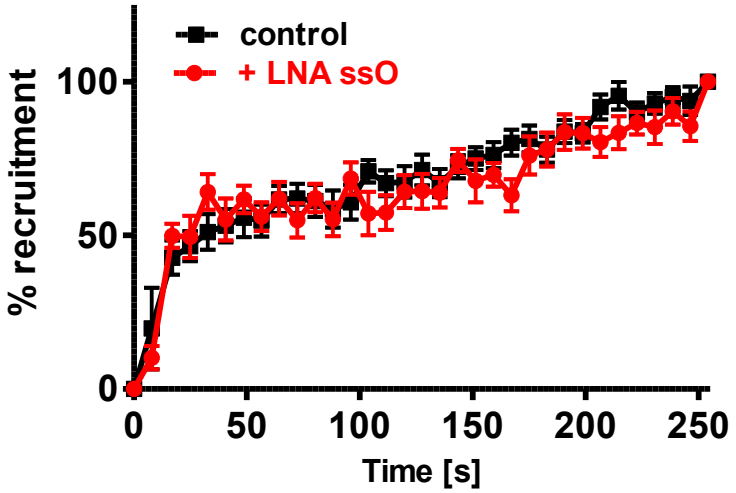

Sup Figure S5